Global NEST Journal, Vol 24, No 3, pp 544-552

Advanced deep learning method for aerial image segmentation of landscape changes in pre- and post-disaster scenarios

Pushpa Latha C.[1]* and Dr. Ajith Bosco Raj T.[2]
[1]Department of Computer Science and Engineering, Arunachala College of Engineering for Women, Kanyakumari, India
[2]Department of Electronics and Communication Engineering, PSN College of Engineering and Technology, Tirunelveli, India
Received: 29/07/2022, Accepted: 20/09/2022, Available online: 27/09/2022
*to whom all correspondence should be addressed: e-mail: pushpalathac1256@gmail.com
https://doi.org/10.30955/gnj.004413

Graphical abstract

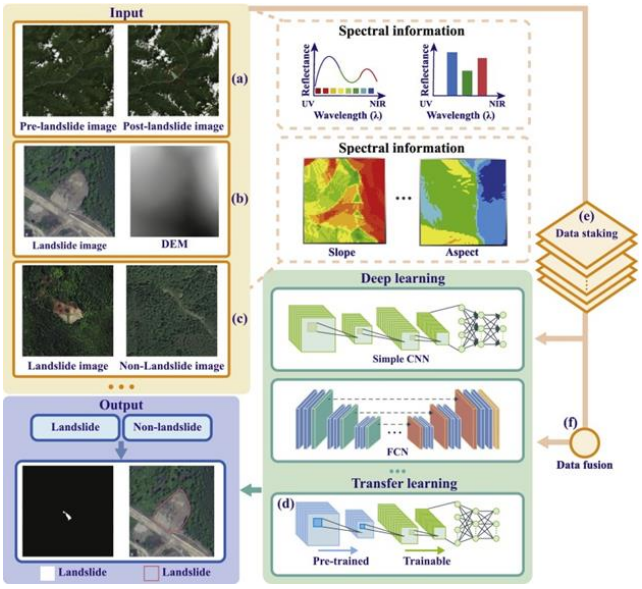

Abstract

The precise analysis of conditions in the landscape before and aftermath of the disaster is a mandatory challenge in aerial image landscape monitoring. The change in patterns of landscape, damaged pathways, and damaged areas will have a major impact without monitoring and redevelopment. Therefore, semantic segmentation of the landscape is required to analyze the changes and avoid other risks in pre-and post-disaster scenarios. To address these queries a deep learning-based landscape monitoring method is presented in this work. A Gated Shaped Convolution Neural Network is utilized for the semantic segmentation of aerial landscape images. Initially, the aerial image undergoes pre-processing with the process of dilation and GSCNN emphasizes the shape and boundary masks of the affected landscape. To choose the best possible pathways and solutions for development the GSCNN undergoes particle swarm optimization. In the current research work, the proposed PSO-GSCNN is evaluated by comparing the accuracy, precision, and recall of the proposed method with Restricted Boltzmann Machines (RBMs), Convolutional Neural Networks, and Fuse-Net segmentation methods. In comparison with conventional RSM, CNN, and Fuse-Net, the accuracy rate of the model is 97.65%, the precision rate is 98.21%, and the recall rate is 97.23%. This technique has achieved 97.66% accuracy, 97% precision, and 96% recall, all higher than the existing methods.

Keywords: Landscape monitoring, aerial image, deep learning, gated shaped convolution neural network, particle swarm optimization

1. Introduction

Landscape monitoring refers to the monitoring of specific landscape areas over time by an ongoing, long-term surveillance system. If timely counteractions are to be taken, appropriate monitoring results in early recognition of crucial changes in the landscape (Sun *et al.*, 2022). Landscape monitoring is a most important application to identify and emphasize the condition of the landscape at different times (Fu *et al.*, 2021). It is mostly tender to early analysis of changes that are to occur in the environment and the emphasis on the after-effects of that change (Syrbe *et al.*, 2007). The aerial image takes a contributed role due to its ability to identify sites, monitor changes in landscape topography through time, and even uncover subsurface features by studying topsoil characteristics and stereoscopic images, aerial photography is widely used in archaeological prospection (Rasidah Hashim 2010). Also, the method gathers important land use information (Hoshi *et al.*, 2014 and Panagopoulos 2008). The aerial image contributes a major role in disaster management and provides adequate information in the form of an image. Aerial image monitoring offers major help in analyzing the landscape areas which have endured the disaster i.e., such areas may develop damaged routes, destruction in such areas due to the disaster (Bila *et al.*, 2011, Aziz *et al.*, 2019 and Courtrai *et al.*, 2016). So, landscape monitoring using any kind of aerial imagery is a mandatory function for further management of such areas after the disaster occurs (Mnih et al 2010). It is hard to observe the changes caused in the landscape manually and the manual analysis consumes complex time and is more susceptible to faults (Kaiser *et al.*, 2017 and Awad

2013). as most of the volunteers may not be competent and experienced in precise analysis. Thus, imaging equipment that widely pictures the large coverage area is needed in monitoring the affected landscape. The precise picturing of the landscape must undergo segmentation of the aerial image to enable precise emphasis of the landscape to obtain the structural changes in patterns in the landscape (Boesch *et al.*, 2008 and Mesquita *et al.*, 2019).

Several prior-art methods are implemented in segmenting the aerial image for disaster management and post-disaster investigation using several techniques and methods. Long-term monitoring of landscape using the aerial image to analyze the change in the landscape by monitoring over a long time has been established by Nor Rashida Hasim (Islam *et al.*, 2022). The land use for cultivation has been monitored by aerial imaging classification. But the work should include further segmentation of the landscape. Also, the classification of the aerial image through the combined action of a modified Support vector machine (SVM) and least square techniques for the monitoring of environmental, land use and further applications. But the drawback is stated that the individual implementation would give better results instead of the combined action of the mechanism. The analysis of the landscape image after a disaster is a crucial role in landscape monitoring by segmenting the landscape images. The lack of segmentation of landscape images may result in misprediction of the changes which may result in severe future issues. To avoid this an advanced deep learning strategy is used in this work for the precise segmentation of the landscape aerial image for better prediction of before and after-effects of the disaster providing timely and actionable information. The following are the main contribution of this paper:

- The Inria aerial image dataset is collected and pre-processed using morphological dilation and corrosion is used to remove noise from aerial data.
- An efficient Particle Swarm Optimized-Gated Shape Convolutional Neural Network is developed for segmentation of the Landscape aerial image which results in efficient segmentation.
- The efficiency of the proposed framework is estimated using precision, accuracy, and recall.
- The results of the proposed method are evaluated based on the comparative analysis with existing Fuse-net, CNN and RBN methods.

The landscape monitoring process is demonstrated as follows, the following section contributes landscape monitoring and segmentation-related research and its drawbacks of the prior art techniques. In the proposed section the elaborate presentation of the proposed GSCNN for semantic segmentation is established followed by the PSO optimization. In the result section, the output processing of the aerial images with the performance analysis of the proposed method with pre-existing techniques is mentioned. Finally, in section 5 the overall study is briefly concluded.

2. Literature review

The antique landscape monitoring techniques have shown drawbacks and issues and further enhancement in the segmentation process. So the review of such pre-existing research is presented in this section.

Andreas Kamilaris and Francesc X. Prenafeta-Boldú (2018) established landscape monitoring using UAVs for the analysis of conditions in the landscape. The situation in the specific area has been viewed through aerial imaging. The process of the work mainly depends on the disaster monitoring and prediction of the disaster by precise monitoring of the landscape. But the process indicates a major drawback in the slow process of monitoring and a large dataset makes the process complex with the prediction of noise in the aerial images captured during monitoring.

Saramsha Dotel et al (2020) proposed a deep learning-based landscape monitoring strategy for disaster management. The regions and landscapes affected and changes have been emphasized by the monitoring strategy. The CNN methodology deals with the semantic segmentation of the captured imagery during pre and post-disaster analysis. But further enhancement in the work has to be done by including object detection and automatic detection of the conditions in the landscape during the disaster by proper alignment of the input dataset to make robust access to the information.

An aerial imagery-based disaster monitoring using deep learning methodology has been established by Siti Nor Khuzaimah Binti Amit and Yoshimitsu Aoki (2017) The wide view of the landscape and the conditions have been monitored using satellite imagery. The early detection and aftereffects and land pattern analysis has been established in the work. The data regarding the real state of the landscape. Further enhancement in the work has to be enabled by inducing the routing procedure analyzed using aerial imaging equipment which is included as a drawback.

Hysa and Fatma Aycim Turer Baskaya (2019) proposed a planning strategy for the landscape to prevent the effects of the disaster. A mental map of urban legibility in disaster studies has appeared to be a useful tool for estimating the behavior of disaster victims in emergencies. For disaster-sensitive spatial designs, as well as for the placement of awareness-raising features in these sites, it's crucial to show how they'll act, the landmarks they'll use for orientation, and the places they'll evacuate to have been utilized by such imaging. Also, mitigating the effects of climate change can be accomplished through enhancing awareness of daily landscapes. But the work has to be enhanced by inducing early prediction of disaster and enabling a disaster-free environment.

R. Monika et al (2018) established a duo strategy of BCS (block comprehensive de-noising) with CTWT (curvelet transform with wiener filtering). A block-wise sampling for compression of data to transmit efficient satellite images has been employed. The restoration of satellite images for effectual de-noising with the proposed approach has been

utilized. The rehabilitation occurs with limited dimensional values. The limitation of the proposed work includes considerable progression in the feature of the image.

Wenzhong Shi et al. (2020) established a review on change detection in remote sensing applications. Artificial intelligence-based change detection research and its innovative role of it in change detection have been expressed in the work. As remote sensing has a major role in the monitoring of the environment, urban planning, and disaster management, the changes in them have to be emphasized so the survey over the various change monitoring has been studied. The research on change detection has to be further enhanced by analyzing additional data about unsupervised AI monitoring, big data monitoring and more.

Xin Gao et al. (2022) have proposed an aerial image-based object detection strategy in low-resolution imagery. Small object detection in the aerial image with the low resolution has been done by the post-processing of the aerial image using the integration of diverse post-processing methodologies. In addition, various vehicle detection methods were implemented for the precise detection of small objects and extraction of specific features from the aerial image. But further enhancement in the detection lacks the precise identification of objects using the automated detection schemes.

Ananya Gupta et al. (2021) implemented a deep learning-based precise segmentation of aerial images for disaster management. The training of the Image-net results in capturing the disaster areas and using the open data it provides the specific data related to the management of disaster and emphasizes the damaged and affected areas. Further enhancement in the work has to be done by implementing the analysis of the road connectivity damages, block in the roads and condition of the landscapes.

According to the literature study, an essential difficulty in aerial image landscape monitoring is the precise analysis of the landscape's state both before and after a disaster. Without monitoring and redevelopment, the altered patterns of the landscape, damaged pathways, and damaged places will have a significant impact. To overcome these challenges PSO-GSCNN methodology has been proposed and is presented in the following section.

3. Proposed PSO-GSCNN method

In this proposed work efficient monitoring of the landscape and enabling information regarding the conditions of the landscape affected due to the disaster is presented and the following flow diagram (Figure 1) indicates the overall process of the proposed work.

The original dataset with no obstacles (i.e., before the disaster) and the dataset with the problem domain (i.e., after the disaster the changes in the patterns of the landscapes and queries) are trained such that, it undergoes further processing.

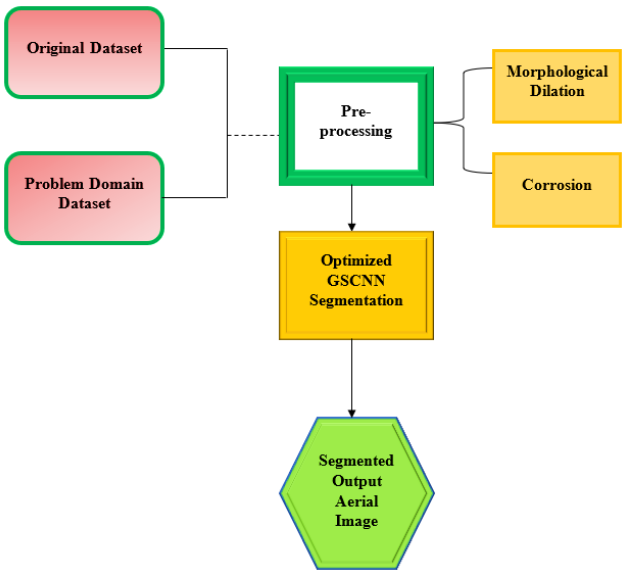

Figure 1. Overall block diagram of the proposed methodology.

3.1. Preprocessing

The initial step includes the pre-processing of the aerial imagery which is an important step for the reduction of unwanted distortion and noise in the imagery. In this research, morphological dilation and corrosion are used to remove noise from aerial data. In aerial images, morphological processes extract structural information to detect landscape area borders. In morphological operations, a structural element is added to an input image to create a corresponding output resulting image. A matrix that identifies the treated pixel in the image and specifies the neighboring pixel value used for processing each pixel is referred to as a structuring element. The dilation process in which the dilation of X by Y is represented by,

$$X \oplus Y = \left\{ z \,|\, (Y)_z \cap X \neq \varnothing \right\} \tag{1}$$

In this case, the structural element X and ∅. denotes the empty set are the same. In other words, the dilation of X by Y is the collection of all the structural element origin positions where the reflected and translated Y overlaps X to some extent.

$$X \,!\; Y = \left\{ z \,|\, (Y)_z \cap X^c \neq \varnothing \right\} \tag{2}$$

When the translated Y does not overlap with the foreground of X, the erosion of X by Y is the collection of all origin locations of structural elements.

3.2. Segmentation via gated shape convolutional neural network

Gated convolutional layers are used to wire boundary information from the intermediate layers of the regular stream's encoding path to the edge stream wch focuses on boundary segmentation solely. The edge stream learns to predict quality edges and uses the Sobel gradient magnitudes of the input image to further highlight contours and textures. Information between the two parallel streams is fused at the end to obtain enhanced boundary predictions. For a semantic segmentation of the landscape aerial image captured in pre-and post-disaster

scenarios, we induced the GSCNN method. The structure of the GSCNN method is depicted in Figure 2.

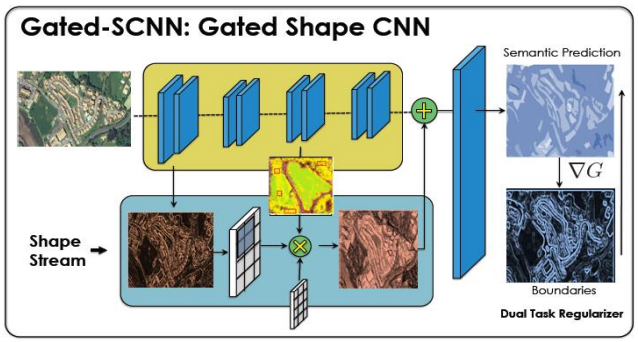

Figure 2. Structure of GSCNN.

The older Gated convolution network comprises the encoder and a decoder section. But this proposed framework comprises of regular and shaped stream accompanied by the fusion module which enables standard segmentation and shape information in the form of boundaries respectively. The shape stream deals with providing relevant data about the landscape boundaries via the gated convolution layer and basic monitoring. Consequently, refined segmentation around boundaries by merging characteristics from both the shape and semantic streams is carried out. Next, each module is presented in detail.

In the proposed architecture, (Figure 3) there are two primary streams: a standard stream and a shaped stream. Any backbone design may provide regular streams. Residual blocks and gated convolutional layers are used to process shapes (GCLs). Using the Atrous Spatial Pyramid Pooling Module, the data from the two streams are then combined on many scales (ASPP). Automated Dual-Task Regularizes assure high-quality border segments in the segmentation mask.

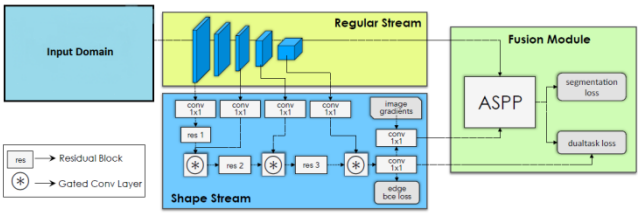

Figure 3. The comprehensive framework of the proposed GSCNN.

Regular stream: The stream $RS_{\theta}(AI)$. takes an image $AI \varepsilon RS^{3\times H\times W}$. with a height H and width W as input and creates dense pixel characteristics, as given by the parameter θ. As the normal stream, any fully-convolutional feedforward network can be employed, such as a ResNet-based semantic segmentation network or a VGG network-based one. For regular-stream segmentation, ResNet-101 and WideResNet are the state-of-the-art. For semantic segmentation, ResNet-101 and WideResNet are the state-of-the-art. Regular streams are represented by their output characteristics, $rs \varepsilon RS^{C\times\frac{H}{f}\times\frac{W}{f}}$. where f is the stride dotes the stride of the stream.

Shape stream: It is represented by the symbol $SS_{\varnothing}$, outputs semantic boundaries with parameters $\varnothing$ after receiving as inputs picture gradients, ∇AI and the result of the first convolutional layer from the regular-stream. In the network design, a few leftover blocks are sandwiched between gated convolution layers (GCLs). As indicated below, GCL ensures that the shape stream only analyses boundary-relevant data (Figure 2). The output boundary map of the shape stream is denoted by the abbreviation $\varepsilon RS^{H\times W}$. We apply supervised binary cross-entropy loss on output borders to supervise the shape stream s GT semantic segmentation masks can be used to obtain Ground-Truth (GT) binary edges.

Fusion Module: The parameters F_{∞}, for fusing the dense feature representations *s* from the regular branch with the boundary representations s from the shape branch in a way that retains multiscale contextual information are supplied as part of this module. By mixing region and boundary characteristics, it generates a finer semantic segmentation K prediction of K semantic classes. The categorical distribution $f=p(y|ss,rs)=F_{\infty}(ss,rs)\int\int R^{N\times H\times W}$ produced by segmentation prediction for an N-class segmentation reveals how probable it is that a pixel belongs to that class among the N classes. To integrate ss and rs, we employ a boundary map in our spatial pyramid pooling approach. This strategy allows for the maintenance of context information at various levels and is a vital component of modern semantic segmentation networks.

3.2.1. Gated convolutional layer

A novel GCL layer is employed to promote information flow from the regular stream to the shape stream since predicting semantic segmentation and semantic boundaries are activities that are closely related to one another. The key element of the suggested architecture, GCL, aids the shape stream in processing the important data by removing the irrelevant data. Features from the regular stream are not included in the shape stream. Instead, it makes advantage of GCL to deactivate its activations that are not considered important by the higher-level data in the regular stream. This may be compared to a two-stream collaborative approach in which the more powerful stream with a deeper awareness of the problem assists the less experienced stream in focusing just on the essential aspects. As a result, the shape stream can adopt a shallow architecture and analyze a very high-resolution image.

Here among two streams, GCL is employed at several locations. Let 't' be the no. of locations, t ∈ 0, 1, · · ·,l the running index, and rs_t and ss_t be the preliminary representations of the relevant regular and shape streams as evaluated by the GCL in the following. To use GCL, an attention map $\gamma_t \varepsilon R^{H\times W}$ is constructed by concatenating rt and st. Then, a sigmoid function σ is introduced, followed by a normalized 1 × 1 convolutional layer $C_{1\times1}$:

$$\gamma_t = \sigma\left(C_{1\times1}\left(ss_t \,||\, rs_t\right)\right) \tag{3}$$

The concatenation of feature maps is referred to as ||, and GCL is implemented as e_t with a component-wise product with an attention map γ_t, accompanied by residual connections and channel-wise weighting with kernel k_t, according to the attention map γ. At each pixel (i, j), a GCL # is calculated as follows:

$$\hat{e}_t^{(i,j)} = \left(e_t \# k_t\right)_{(i,j)} = \left(\left(e_{t(i,j)} \square \gamma_{t(i,j)}\right) + k_{t(i,j)}\right)^T k_t \quad (4)$$

$\hat{e}_t$ is sent on to be further processed in the shape stream's subsequent levels. Backpropagation is possible in both attention map computation and gated convolution because the calculations are distinct. Instinctively, γ is be considered as an attention m that lends more weight to places with crucial border information from the perspective of an attention map. In our research, we employed three different GCLs. These are connected to the standard stream's third, fourth, and fifth layers. Bilinear interpolation is being used to up-sample the feature maps from the normal stream if necessary.

3.2.2. Joint multi-task learning

Apart of an end-to-end strategy, we learn the regular and shape streams along with the fusion module. Supervised segmentation and boundary map prediction are combined in the training phase. We employ typical binary cross-entropy (BCE) loss to determine the expected boundary maps s and the predicted semantic segmentation f.

$$L^{\theta\varnothing\propto} = \lambda_1 L_{BCE}^{\theta,\phi}\left(e,\hat{e}\right) + \lambda_2 L_{CE}^{\theta,\phi}\left(\hat{y},f\right) \quad (5)$$

The boundaries of GT are denoted by $\hat{e}_\varsigma R^{H\times W}$, and the semantic labels by $\hat{y}_\varsigma R^{H\times W}$. The weighting of the losses is controlled by two hyperparameters, λ_1. and λ_2. As well as regular stream parameters, the BCE loss $L_{BCE}^{\theta,\phi}$. BCE updates shape stream parameters. We update all network parameters at the end of the final categorical distribution of semantic classes with CE loss $L_{CE}^{\theta,\phi}$, as in standard semantic segmentation networks. The significant difference between a boundary and non-boundary pixels on boundaries in BCE is taken into account using the β coefficient.

3.2.3. Dual task regularizer

As indicated previously, $p(y|ss,rs)\int R^{N\times H\times W}$ is a categorical distribution generated by the fusion module. Let $\delta\int R^{H\times W}$ be the potential that indicates if a particular pixel is part of a semantic boundary in the image. The following spatial derivative is calculated based on segmentation output:

$$\delta = \frac{1}{\sqrt{2}} |\,|\nabla(G * \arg\max_k p\left(y^N\right) rs, ss\right) \quad (6)$$

where G denotes Gaussian filter.

The overall loss is denoted as,

$$Loss = \lambda_1 * L_{semantic} + \lambda_2 * L_{edge} + L_{dualtask} \quad (7)$$

Even though, the proposed GSCNN enables the precise masking of the boundaries and shapes, the best possible choice of the pathways and solutions are addressed by optimizing the proposed method with PSO.

PSO optimization: PSO has been suggested by Eberhart and Kennedy in 1995. It has been used vastly in the last two decades. It is an easily accessible technique for resolving complex optimization problems. The concept of PSO has been adopted from the biological behavior of swarms of birds. The benefits of the PSO algorithm include the rapid convergence rate, easiness, and good accuracy for solving non-linear, and discrete problems by choosing the best solution. With the aid of PSO, the research expects to fine-tune GSCNN hyperparameters including learning rate, momentum, and weight decay. When optimizing the network's weights, PSO employs these parameters as the objective criterion in the loss function, however, they can be difficult to get since they are often application-dependent, whereas GSCCNN is the objective criterion to minimize. Particle Swarm Optimization will identify the ideal hyper-parameter values in this way, minimizing the loss of functions throughout the training set. Firstly, the initialization is done with the particles with random values for each component of the solution vector. The efficiency of each particle is then determined based on its characterization of a solution. If the current solution fitness is better than the *pbest,* the existing solution will be updated with the current solution. If the existing solution's fitness is better than *gbest*, the current solution will be updated with gbest as well. *Xi = (X1, X2,..., Xin), Vi = (V1, V2,..., Vin)*, and *Pi = (P1, P2,..., Pin)*, which are n-dimensional vectors denoting the i-th particle's velocity as well as the particle's previously best location, *I = 1,2,..., N*, and *t = 1, 2,..., T*, are used in this equation. Its parameter is regulated by w; its cognitive and social learning rates are controlled by c1 and c2; a random number and a random number, respectively, offer variety to the population; its best particle index is g; its constriction factor X controls the size of the velocity. The iteration cycle is repeated until the halting requirement is reached, which might take multiple iterations or a good solution. Another technique may be added to PSO to boost its performance even further. The swarm is extinguished and PSO is rebuilt while preserving *gbest*, resulting in swarm diversification, also known as an explosion. The particles' new velocities in the search space are then estimated using Eq 1. The search procedure for an optimum value has been continued till the termination criterion has been reached. The velocity and position of the particles have been evaluated as follows.

$$V_i^{k+1} = WV_i^k + C_1 r_1 (P_{best_i} - P_i^k) + C_2 r_2 (G_{best} - P_i^k) \quad (8)$$

and

$$P_i^{k+1} = P_i^k + V_i^{k+1} \quad (9)$$

V_i^k , P_i^k velocity, the position of particle *i* at iration *k*

V_i^{k+1} ,. P_i^{k+1} velocity, location of particle *i* at iteration *k*

P_{best_i} the best location of particle *i* until ition *k*
G_{best} global best location
i position of the particle
W inertia weight
C_1, C_2 local weight
r_1, r_2 random variables evenly dispersed inside [0,1]
K iteration number

Thus, the PSO-Optimized GSCNN enables the precise monitoring and segmenting of the specific areas and conditions in the disaster landscape by the best possible prediction using semantic segmentation. The following section deals with the demonstration of the result and performance analysis of the proposed work.

4. Result and discussion

In this section performance of the proposed PSO-Optimized GSCNN algorithm is analyzed and assed with other existing methods. The findings by experimenting with our GSCNN architecture used diverse types of disasters using Inria aerial image dataset. The comprehensive processing of the proposed method is carried out concerning the respective disaster such as hurricane, flood and tsunami aerial imagery. The output of the proposed work is demonstrated as follows,

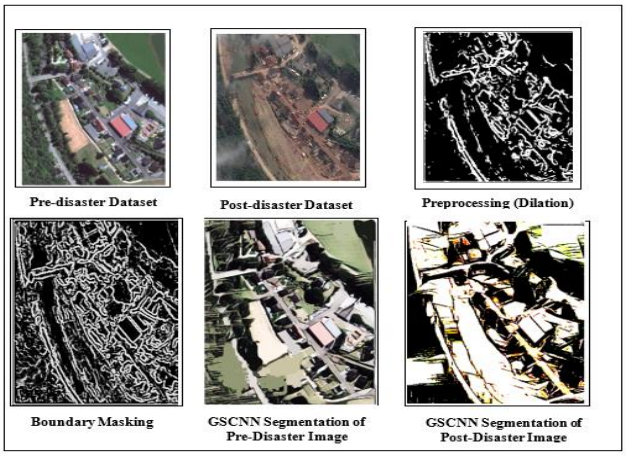

Figure 4. Proposed semantic segmentation of hurricane landscape.

The pre-disaster dataset and post-disaster dataset trained in the labeling dataset undergo the pre-processing process to remove the redundant data present in the aerial image. Further the boundary and shape masking to undergo the semantic segmentation is carried out. Finally, the PSO-optimized GSCNN deals with the segmentation of both the pre-and post-disaster dataset to emphasize the changes and destruction and damaged roads, and pathways in comparing both. The efficient segmentation is carried out and respective states and changes are emphasized. Figures 4–6 represent the output representation of semantic segmentation of landscape aerial images of disasters such as hurricanes, Flood and tsunamis respectively.

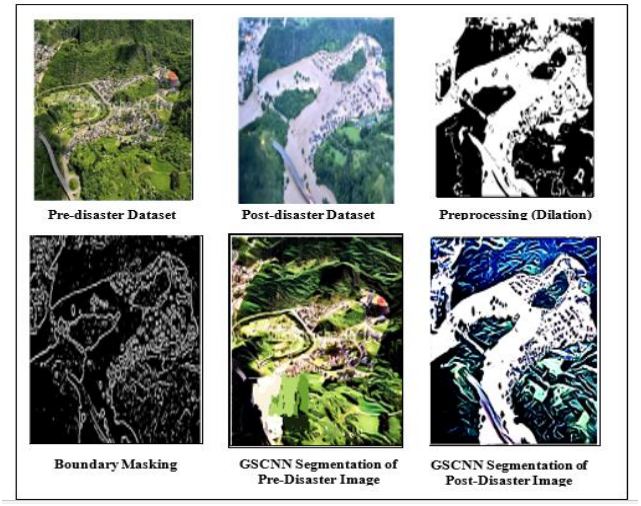

Figure 5. Proposed semantic segmentation of flood landscape.

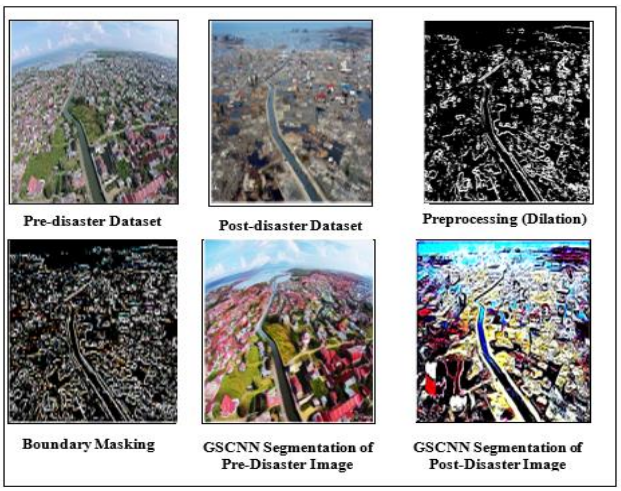

Figure 6. Proposed semantic segmentation tsunami landscape.

4.1. Evaluation indicators

To delineate the GSCNN model performance loss function and accuracy are analyzed with existing models. The PSO-GSCNN semantic segmentation model performance is analyzed by Precision (P), recall(R), Accuracy and PR curve. Where Precision is the consistency between the detected landscape area and the real landscape area. The recall is the proportion of the correct segmentation of samples in the total Sample.

$$P = \frac{TP}{TP + FP} \tag{10}$$

$$R = \frac{TP}{TP + FN} \tag{11}$$

Where True positives (TP) represent the model that correctly predicted disaster areas in the landscape, True negative (FN) is the proposed model that does not predict landscape disaster areas, and FP(False Positive) are cases in which the network predicts the disaster areas incorrectly.

$$A = \frac{f}{N} \quad (12)$$

Here f is the no. of corrected predictions and N is the no. of samples.

The performance of the proposed method is evaluated based on the comparison of the suggested method with prior-art methods. The comparison of the accuracy, precision and recall of the proposed PSO-GSCNN is analyzed with Restricted Boltzmann-machine (RBM) [Sublime *et al.*, 2019], Convolution Neural Network [Dotel *et al.*, 2020] and Fuse-Net [Persello *et al.*, 2021] segmentation techniques. Figure 7 shows the accurate comparison of the suggested method with existing models

Table 1. Comparative analysis of accuracy

Techniques	Accuracy
RBM	94
CNN	92
Fuse-Net	96
PSO-GSCNN	98

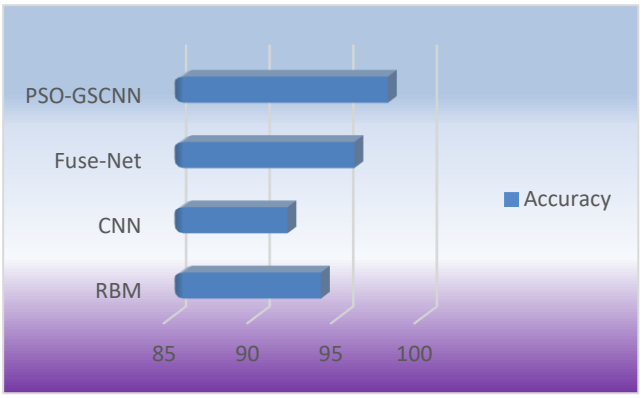

Figure 7. Accuracy comparison with existing models.

Table 1 shows the accuracy performance of the PSO-GSCNN of different landscape segmentation. The accuracy rate of the model is 97.65% which is significantly high compared to the existing segmentation methods.

Table 2. Comparative analysis of precision

Techniques	Precision
RBM	92
CNN	91
Fuse-Net	95
PSO-GSCNN	99

Table 2 shows the precision performance of the PSO-GSCNN of different landscape segmentation. The precision rate of the model is 98.21% which is significantly high compared to the existing segmentation methods. Figure 8 shows the precision comparison of the proposed method with existing models.

Table 3. Comparative analysis of precision

Techniques	Recall
RBM	90
CNN	95
Fuse-Net	93
PSO-GSCNN	98

Table 3 shows the Recall performance of the PSO-GSCNN of different landscape segmentation. The recall rate of the model is 97.23% which is significantly high compared to the existing segmentation methods. Figure 9 shows the recall comparison of the proposed method with existing models.

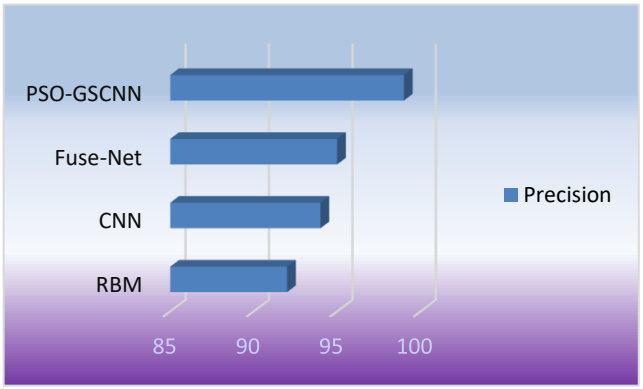

Figure 8. Precision comparison with existing models.

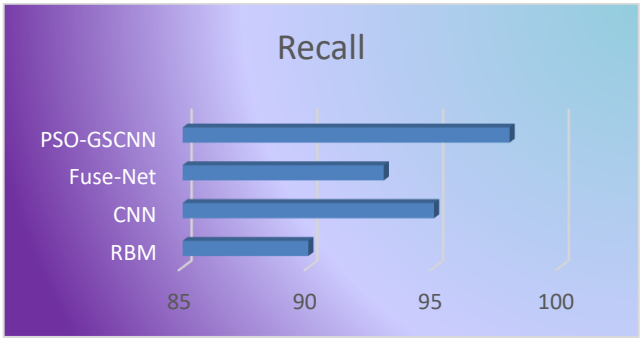

Figure 9. Precision comparison with existing models.

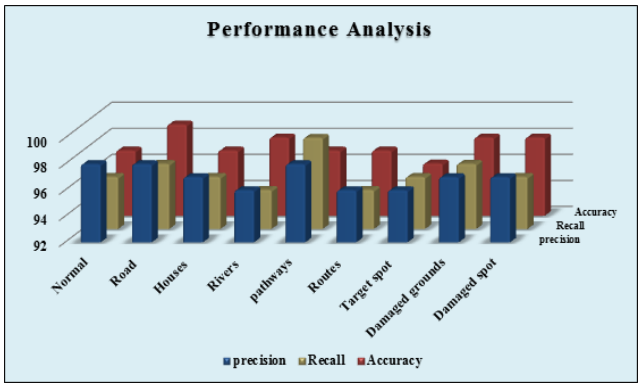

Figure 10. Overall performance measure.

Table 4. Overall performance analysis based on different classes of the landscape

Class	Precision (%)	Recall (%)	Accuracy (%)
Normal	98	96	97
Road	98	97	99
Houses	97	96	97
Rivers	96	95	98
pathways	98	99	97
Routes	96	95	97
Target spot	96	96	96
Damaged grounds	97	97	98
Damaged spot	97	96	98
Average	97	96	97.66

The overall performance of the proposed method is analyzed by the accuracy, precision and recall calculation in terms of the state of the landscape concerning normal landscape, road, houses, rivers, pathways, routes, target spots, damaged grounds and damaged spots of the monitored landscape affected by the disaster. The average accuracy occurred is 97.66%, the average precision is achieved by 97% and the average recall is attained by 96%. Figure 10 indicates the graphical representation of the overall performance analysis based on the different classes of the landscape.

Table 4 shows the performance of the proposed system with the different classes of the landscape affected by the disaster. The average accuracy of the model is 97.65% which is significantly high compared to the segmentation techniques.

5. Conclusion

This research presents a deep learning-based landscape monitoring method for the semantic segmentation of aerial landscape images, using a Gated Shaped Convolution Neural Network. Aerial images undergo pre-processing with the process of dilation and GSCNN highlighting the shape and boundary masks of the affected landscape. The GSCNN undergoes particle swarm optimization to choose the best possible development path. The results of the proposed method are evaluated based on the comparative analysis with prior-art methods. The comparison of the accuracy, precision, and recall of proposed PSO-GSCNN is analyzed with Restricted Boltzmann Machine (RBM), Convolution Neural Network and Fuse-Net segmentation techniques. The accuracy rate of the model is 97.65%, the precision rate of the model is 98.21%, the recall rate of the model is 97.23% in comparison with the conventional RSM, CNN and Fuse-Net respectively. The average accuracy occurred is 97.66%, the average precision is achieved by 97% and the average recall is attained by 96 % which is higher compared to the existing techniques.

Acknowledgment

The authors with a deep sense of gratitude would thank the supervisor for his guidance and constant support rendered during this research.

Funding statement

The authors received no specific funding for this study.

Conflicts of interest

The authors declare that they have no conflicts of interest to report regarding the present study.

References

Amit S.N.K.B. and Aoki Y. (2017). Disaster detection from aerial imagery with convolutional neural network. In International Electronics Symposium on Knowledge Creation and Intelligent Computing (IES-KCIC), pp. 239–245.

Awad M.M. (2013). A morphological model for extracting road networks from high-resolution satellite images. Journal of Engineering, **2013**, 1–9.

Aziz A. and Anwar M.M. (2019). Landscape change and human environment. *Environment, Earth and Ecology*, **3**, 7–12.

Bila J., Jura J. and Bukovsky I. (2011). Qualitative modeling in the landscape development monitoring, landscape, **27,** 26–35.

Boesch R. and Wang Z. (2008). Segmentation optimization for aerial images with spatial constraints. Proceeding of The International Archives of the Photogrammetry, Remote Sensing and Spatial Information Sciences, **37**, 285–290.

Courtrai L. and Lefèvre S. (2016). Morphological path filtering at the region scale for efficient and robust road network extraction from satellite imagery, Pattern Recognition Letters, **83**, 195–204.

Dotel S., Shrestha A., Bhusal A., Pathak R., Shakya A. and Panday S.P. (2020). Disaster Assessment from Satellite Imagery by Analysing Topographical Features Using Deep Learning. In Proceedings of the 2020 2nd International Conference on Image, Video and Signal Processing, Singapore, Singapore**,** pp. 86–92.

Dotel S., Shrestha A., Bhusal A., Pathak R., Shakya A. and Panday S.P. (2020). Disaster assessment from satellite imagery by analysing topographical features using deep learning, In Proceedings of the 2020 2nd International Conference on Image, Video and Signal Processing, Singapore, Singapore, pp. 86–92.

Fu H., Fu B. and Shi P. (2021). An improved segmentation method for automatic mapping of cone karst from remote sensing data based on deeplab V3+ model, Remote Sensing, **13,** 441.

Gao X., Ram S., Philip R.C., Rodríguez J.J., Szep J., Shao S. and Hariri S. (2022). Selecting post-processing schemes for accurate detection of small objects in low-resolution wide-area aerial imagery. Remote Sensing, **14**, 255.

Gupta A., Watson S. and Yin H. (2021). Deep learning-based aerial image segmentation with open data for disaster impact assessment. Neurocomputing, **439**, 22–33.

Hoshi T., Murao O., Yoshino K., Yamazaki F. and Estrada M. (2014). Post-disaster urban recovery monitoring in Pisco after the 2007 Peru earthquake using satellite image, Journal of Disaster Research, **9**, 1059–1068.

Hysa A. and Başkaya F.A.T. (2019). A GIS based method for indexing the broad-leaved forest surfaces by their wildfire ignition probability and wildfire spreading capacity. Modeling Earth Systems and Environment, **5,** 71–84.

Islam S.U., Jan S., Waheed A., Mehmood G., Zareei M. and Alanazi F. (2022). Land-cover classification and its impact on peshawar's land surface temperature using remote sensing. Comp. Materials and Continua, **70**, 4123–4145.

Kaiser P., Wegner J.D., Lucchi A., Jaggi M., Hofmann T. and Schindler K. (2017). Learning aerial image segmentation from online maps. IEEE Transactions on Geoscience and Remote Sensing, **55**, 6054–6068.

Kamilaris A. and Prenafeta-Boldú F.X. (2018). Disaster monitoring using unmanned aerial vehicles and deep learning. *arXiv preprint arXiv:1807.11805*.

Mesquita D.B., dos Santos R.F., Macharet D.G., Campos M.F. and Nascimento E.R. (2019). Fully convolutional siamese autoencoder for change detection in UAV aerial images. IEEE Geoscience and Remote Sensing Letters, **17,** 1455–1459.

Mnih V. and Hinton G.E. (2010). Learning to detect roads in high-resolution aerial images. In European conference on computer vision. Berlin, Heidelberg. 210–223.

Monika R., Anilet Bala A. and Suvarnamma A. (2018). Block compressive sampling and wiener curvelet denoising approach for satellite images. In International Conference on Intelligent Computing and Applications, Springer, Singapore, pp. 11–18.

Panagopoulos T.H.O.M.A.S., Blumberg D.O. and Orlovsky L. (2008). L. Monitoring the Aral Sea landscape change. In Proceedings of the 4th WSEAS International Conference on Energy, Environment, Ecosystems & Sustainable Development, Algarve, Portugal, 254–258.

Persello C., Wegner J.D., Hänsch R., Tuia D., Ghamisi P., Koeva M. and Camps-Valls G. (2021). Deep learning and earth observation to support the sustainable development goals. *arXiv preprint arXiv:2112.11367*.

Rasidah Hashim N. (2010). Analysing Long-Term Landscape Changes in a Bornean Forest Reserve Using Aerial Photographs, The Open Geography Journal, **3**, 161–169.

Shi W., Zhang M., Zhang R., Chen S. and Zhan Z. (2020). Change detection based on artificial intelligence: State-of-the-art and challenges. Remote Sensing, **12**, 1688.

Sublime J., and Kalinicheva E. (2019). Automatic post-disaster damage mapping using deep-learning techniques for change detection: Case study of the Tohoku tsunami. Remote Sensing, **11**(9), 1123.

Sun X., Xia M. and Dai T. (2022). Controllable Fused Semantic Segmentation with Adaptive Edge Loss for Remote Sensing Parsing, Remote Sensing, **14,** 207.

Syrbe R.U., Bastian O., Röder M. and James P. (2007). A framework for monitoring landscape functions: The Saxon Academy Landscape Monitoring Approach (SALMA), exemplified by soil investigations in the Kleine Spree floodplain (Saxony, Germany), Remote Sensing, **79,** 190–199.